Journal of Nuclear Medicine, published on August 26, 2021 as doi:10.2967/jnumed.121.262528

Title: Repeatability of ^{68}Ga-PSMA-HBED-CC PET/CT-derived total molecular tumor volume

Short title: Repeatability PSMA total MTV

Robert Seifert[1,2,3], Patrick Sandach[1,2], David Kersting[1,2], Wolfgang P. Fendler[1,2], Boris Hadaschik[2,4], Ken Herrmann[1,2], John J. Sunderland[5], Janet H. Pollard[5,6]

1. Department of Nuclear Medicine, University of Duisburg-Essen and German Cancer Consortium (DKTK)-University Hospital, Essen
2. West German Cancer Center
3. Department of Nuclear Medicine, University Hospital Münster, University Münster, Münster, Germany
4. Department of Urology, University Hospital Essen, Essen, Germany and German Cancer Consortium (DKTK)-University Hospital, Essen
5. Department of Radiology, University of Iowa Carver College of Medicine, Iowa City, Iowa
6. Department of Radiology, Iowa City Veterans Healthcare Center, Iowa City, Iowa

Keywords: PSMA PET; tumor volume; repeatability

Word count: 5078

Corresponding author:

Robert Seifert, MD

Hufelandstraße 55, 45147 Essen, Germany

Phone: +49 201 723 2032

Fax: +49 201 723 5658

E-mail: robert.seifert@uk-essen.de

Abstract

Background

Molecular tumor volume (MTV) is a parameter of interest in ~~advanced~~ prostate cancer for assessing total disease burden on prostate-specific membrane antigen (PSMA) PET. Although software segmentation tools can delineate whole-body MTV, a necessary step towards meaningful monitoring of total tumor burden and treatment response through PET is establishing the repeatability of these metrics. The present study assesses the repeatability of total MTV and related metrics for ^{68}Ga-PSMA-HBED-CC in ~~advanced~~ prostate cancer.

Methods

Eighteen patients from a prior repeatability study who underwent two test-retest PSMA PET/CT scans within a mean interval of 5 days were reanalyzed. Within subject coefficient of variation and repeatability coefficients (RC) were analyzed on a *per lesion* and *per patient* basis. For the *per lesion* analysis, individual lesions were segmented for analysis by a single reader. For *per patient* analysis, subgroups of up to 10 lesions (single reader) and the total tumor volume per patient were segmented (independently by two readers). Image parameters were: MTV; maximum, peak, and mean standardized uptake value; total lesion PSMA and the related metric PSMA quotient (which is integrating lesion volume and PSMA avidity).

Results

In total, 192 segmentations were analyzed for the *per lesion* analysis and 1662 segmentations for the total tumor volume *per patient* analysis (combining the 2 readers and 2 scans). The RC of the MTV of single lesions was 77% (95%CI:63-96%). The RC improved after aggregation of up to 10 manually selected lesions into subgroups assessed *per patient*, 33% (95%CI:25-46%). The RC of

the semi-automatic MTV_{total} was 35% (95%CI:25-50), the bland-altman bias was -6.70 [95%CI:-14.32 – 0.93]. Alternating readers between scans led to a comparable RC of 37% (95%CI:28-49%) for MTV_{total} meaning that the metric is robust between scanning sessions and between readers.

Conclusion

^{68}Ga-PSMA-HBED-CC PET-derived semi-automatic MTV_{total} is repeatable and reader independent with a change of ±35% representing a true change in tumor volume. Volumetry of single manually selected lesions has considerably lower repeatability, and volumetry based on subgroups of these lesions, while showing acceptable repeatability, is less systematic. The semi-automatic analysis of MTV_{total} employed in this study offers an efficient and robust means of assessing response to therapy.

Introduction

Prostate cancer is a leading cause of death in men (*1*). Especially in advanced prostate cancer, therapy monitoring is challenging. The blood tumor marker prostate-specific antigen (PSA) is routinely used to monitor disease progression (*2*). However, PSA levels may be influenced by tumor dedifferentiation and androgen deprivation therapy, which raises the need for image-based methods for global tumor assessment (*3*,*4*). For now, bone scan and computed tomography (CT) are the established methods for assessing treatment response in advanced disease (*2*). More recently, the prostate-specific membrane antigen (PSMA) imaging with positron emission tomography (PET) has been shown to be superior both for initial and recurrent cancer staging compared to conventional imaging (*5*,*6*). Therefore, PSMA PET seems to be a promising methodology to quantify the prostate cancer tumor volume over time.

The recently proposed PSMA PET Progression criteria as well as a recently published consensus meeting recommended consideration of PSMA PET-derived volumetric measurements to detect progressive disease (*7*,*8*). Indeed, several studies have shown that the quantification of the total tumor volume using PSMA PET is feasible, and that it is a statistically significant negative predictor for overall survival in patients with advanced prostate cancer (*9*–*12*). Total tumor uptake values analogous to total lesion glycolysis for ^{18}F-fluorodeoxyglucose can also be assessed with PSMA PET.

To date the repeatability of PSMA PET-derived volumetric and total tumor uptake measurements have not been sufficiently investigated. Previously Pollard et al. reported ^{68}Ga-PSMA-HBED-CC PET repeatability for SUV_{max} in bone and nodal metastases from prostate cancer (*13*). A variety of factors beyond true change in tumor can lead to variability in quantitative PET imaging, including

the segmentation methods used. To reliably assess quantitative change between PSMA PET scans, it is necessary to understand the normal variability within the patient, radiotracer, and imaging system. The present study evaluates repeatability of volumetric and uptake measurements for individual tumors and total tumor volume on test-retest ^{68}Ga-PSMA-HBED-CC PET/CT.

Methods

Patients and image acquisition

A total number of 18 patients were included in the analysis. Institutional review board (IRB) approved the study protocol (NCT02952469) and all subjects signed a written informed consent. Dataset details were previously reported by Pollard et al. in their study of test-retest repeatability (*13*). Here, the identical dataset was employed. Briefly, all patients underwent two PSMA PET/CT acquisitions within a mean interval of 5 days (range: 2-14 days). Patient characteristics are shown in Table 1. Synthesis of ^{68}Ga-Gallium-PSMA-HBED-CC (also known as PSMA-11 and referred to simply as PSMA in the remainder of this paper) was performed as previously published (*13*). Either a Biograph mCT (with FlowMotion) or a Biograph Truepoint PET/CT system were used for image acquisition (Siemens Healthineers, Knoxville, TN, USA). The follow-up scan was performed on the same scanner as the initial scan. PET data were acquired using a previously published acquisition protocol (PET scan starting 60 minutes after tracer injection with scan coverage from vertex to mid-thigh, 3-4 minutes scan time per bed position) (*13*). A three-dimensional ordered-subset expectation maximization (OSEM) algorithm was used for image reconstruction (with time-of-flight information in case of the mCT).

Tumor analysis *per lesion*

For the repeatability analysis of individual lesions, up to 10 metastases (skeletal or nodal) or primary tumor lesions were segmented both in the first and second scan by a single reader using a manual segmentation with a 50% isocontour. A single reader model was chosen for single lesion and the subgroup analysis portions of the study. Because the same small number of lesions needed to be selected on each PET scan, the single reader approach minimized variability introduced by inter-rater differences in lesions selection and segmentation. Lesions were identified as non-physiologic sites of uptake with an SUV exceeding the regional background activity. Lesions were selected at random from the regions segmented by the whole-body molecular tumor volume analysis described in detail below in the section on total tumor analysis. For each lesion, the maximal, peak, and mean standardized uptake values (lesion SUV_{max}, SUV_{peak}, and SUV_{mean}, respectively), molecular tumor volume (MTV_{lesion}), total lesion PSMA ($PSMA\text{-}TL_{lesion}$), and total lesion quotient ($PSMA\text{-}TLQ_{lesion}$) were measured. MTV_{lesion} was determined by the sum of the voxels (Eq.1) within a threshold 50% isocontour of the local SUV_{max}. $PSMA\text{-}TL_{lesion}$ and $PSMA\text{-}TLQ_{lesion}$ were calculated as in Eq. 2 and 3.

$$MTV_{lesion} = \sum_{i=0}^{total}(voxel_i) \qquad \text{Eq. 1}$$

$$PSMA\text{-}TL_{lesion} = MTV_{lesion} \times lesion\ SUV_{mean} \qquad \text{Eq. 2}$$

$$PSMA\text{-}TLQ_{lesion} = \frac{MTV_{lesion}}{lesion\ SUV_{mean}} \qquad \text{Eq. 3}$$

Tumor subgroup analysis *per patient*

One reader manually selected at random a group of up to 10 lesions *per patient* from the regions segmented by the whole-body MTV analysis technique (described in the next section). In patients

with a large number of metastatic lesions, lesions were selected randomly to reflect a broad distribution of anatomical regions. The lesions in this subgroup were individually manually segmented and were assessed as an aggregate. The mean of SUV_{max} and SUV_{mean} (subgroup meanSUV_{max} and subgroup meanSUV_{mean}, respectively) were calculated. The sum and mean of $MTV_{lesion,}$ the sum of PSMA-TL_{lesion}, and the sum of PSMA-TLQ_{lesion} ($MTV_{subgroup}$, subgroup MTV_{mean}, PSMA-$TL_{subgroup,}$ and PSMA-$TLQ_{subgroup}$, respectively) were calculated as in Eq. 4-7 where *n* is the number of lesions within the subgroup and *i* is the ordinal number of the lesion. PSMA-TL_{lesion} is analogous to total lesion glycolysis for ^{18}F-FDG and when calculated for aggregate tumors the individual PSMA-TL_{lesion} values are summed.

$$MTV_{subgroup} = \sum_{i=1}^{n}(MTV_{lesion\ i}) \quad \text{Eq. 4}$$

$$\text{Subgroup } MTV_{mean} = \frac{\sum_{i=1}^{n}(MTV_{lesion\ i})}{n} \quad \text{Eq. 5}$$

$$\text{PSMA-}TL_{subgroup} = \sum_{i=1}^{n}(\text{PSMA-}TL_{lesion\ i}) \quad \text{Eq. 6}$$

$$\text{PSMA-}TLQ_{subgroup} = \sum_{i=1}^{n}(\text{PSMA-}TLQ_{lesion\ i}) \quad \text{Eq. 7}$$

Total tumor analysis *per patient*

For the total tumor analysis, all lesions were segmented using a semi-automatic approach as previously published (*9*). The investigational MICIIS research software prototype was employed for the single lesion and total tumor analyses (previously named: MI Whole-Body Analysis Suite, MIWBAS, Siemens Healthineers, Knoxville, TN, USA). Briefly, all voxels with SUV_{peak} exceeding the following liver-specific threshold were selected as candidate foci:

$$SUV_{peak}\,\text{threshold} \geq \frac{4.3}{\text{liver SUVmean}} \times (\text{liver SUVmean} + \text{liver SUVstd}) \quad \text{Eq. 8}$$

where the liver-specific threshold was calculated as previously described and SUV_{std} is the standard deviation of the SUV distribution in the liver volume of interest (*9*,*10*). The threshold described in Eq. 8 adjusts for the tumor "sink effect" that has a tendency to lower liver uptake; the first part of the formula is a corrective coefficient for the SUV reduction due to the "sink effect" and the second part is the calculation for the uncorrected liver threshold. Individual lesions were segmented based on a threshold 50% isocontour of the local SUV_{max}. In analogy to the European Association of Nuclear Medicine recommendations for FDG-PET imaging a threshold 50% isocontour-based approach was chosen for this study (*14*). Segmentation errors such as inclusion of sites of normal physiologic uptake or exclusion of tumor lesions were adjusted manually. There were no adjustments of segmented tumor contours in addition to inclusion or exclusion of lesions. Example whole-body tumor segmentations and segmentation errors are shown in **Fig. 1 and 2**. Two readers with PET experience independently performed the delineation of all tumor lesions and their delineated PET data were analyzed separately.

The sum of all voxels in the whole-body total tumor segmentation *per patient* was designated MTV_{total}. The mean of the volume of the individual segmented volumes comprising the MTV_{total} was calculated as in Eq. 5, and designated total MTV_{mean}. Likewise, the mean of SUV_{max} and SUV_{mean} of these component volumes was designated total meanSUV_{max} and total meanSUV_{mean}, respectively. The $PSMA\text{-}TL_{lesion}$ and $PSMA\text{-}TLQ_{lesion}$ values for the component volumes were summed as in Eq. 6 and 7, and designated $PSMA\text{-}TL_{total}$ and $PSMA\text{-}TLQ_{total}$, respectively.

Statistical analysis

Statistical methods for the sample size of the original dataset used in this analysis are reported by Pollard et al (*13*). Pearson correlation coefficient was used for descriptive statistics. Bland-Altman plots were created for absolute (rather than relatively percent) differences in MTV_{total} and

meanSUV$_{max}$ (*15*). Correlation in MTV$_{total}$ between readers for the same scan and between scans for the same reader were evaluated with intraclass correlation coefficients (ICC). The repeatability assessment using a relative comparison approach was done as described by Obuchowski (*16*). The within-subject coefficient of variation (wCV) is given by

$$wCV = \sqrt{\frac{\sum_{i=1}^{n} \frac{(ScanA_i - ScanB_i)^2}{2 \times \left(\frac{1}{2}(ScanA_i + ScanB_i)\right)^2}}{n}} \qquad \text{Eq. 9}$$

where *n* is the number of subjects and *ScanA* and *ScanB* are the quantitative PET measurements from the first and second PET scan, respectively. The repeatability coefficient (RC) is given by

$$RC = 1.96 \times wCV \times \sqrt{2} \qquad \text{Eq. 10}$$

The confidence intervals for wCV and RC were determined by bootstrapping with 1,000 replicates. RC variabiliaty in relation to lesion SUV$_{max}$ was evaluated by an exploratory approach for subsets of lesions in multiple steps. For each step, all lesions which had an SUV$_{max}$ below an arbitrarily defined SUV$_{max}$ threshold were included. A distinct threshold was used for each step, the lowest SUV$_{max}$ threshold was 1, the increment was 5. Statistical analyses were performed using R v3.5.2 (The R Foundation, r-project.org) and Microsoft Excel 2016 v16.0.5110.1000. Statistical analysis was done by D.K. and R.S.

Results

Test-retest scan parameters

As previously published for the same cohort, the median interval between scan 1 and scan 2 was 5 days (2 – 14 days). No statistically significant difference was observed regarding injected dose (mean 133.1 MBq vs. 133.1 MBq, p = 1.0) and image delay (60. 6 min vs. 60.7 min, p = 0.9) between scan 1 and 2. Patient characteristics are shown by Table 1.

Repeatability of manually segmented individual lesions

For the *per lesion* analysis, 96 metastases from 18 patients were manually delineated by a single reader resulting in a total number of 192 segmentations from the two scans. Segmented lesions were regarded as independent observations. The RCs of MTV_{lesion} and related metrics are shown in **Table 2**. Linear regression and Bland-Altman scatterplots for MTV_{lesion} on scan 1 and scan 2 showed relatively strong correlation ($P<0.001$, $R^2 = 0.85$) and no significant bias based on visual analysis (**Fig. 3A and B**). However, MTV_{lesion} demonstrated poor repeatability with RC 76.9% [95%CI:62.9 – 95.9 %] and similarly poor repeatability when accounting for differences in lesion volume with RC 64.7% [49.3 – 91.6%] for lesions ≥ 5 ml and 83.9% [65.5 – 110.7 %] for lesions < 5 ml. The Bland-Altman bias of MTV_{lesion} was -0.39 [95%CI: -1.00 – 0.22] for all lesions. The deviation of MTV_{lesion} between scan 1 and scan 2 was statistically significantly correlated with the deviation of SUV_{max} between scan 1 and 2 ($p < 0.001$, $R^2 = 0.17$) (**Fig. 3C**).

Repeatability of manually segmented subgroup of lesions per patient

Given the poor repeatability of MTV_{lesion}, a larger subgroup of manually selected and segmented lesions was evaluated for repeatability *per patient*. Inclusion of multiple lesions for assessment as a subgroup allows for mitigation of individual lesion variability by averaging positive and negative

variation across a larger number of lesions. The repeatability of $MTV_{subgroup}$ and related metrics are presented in **Table 3**. $MTV_{subgroup}$ demonstrated improved repeatability with RC 33.1% [95%CI:24.2 – 46.2%] compared to MTV_{lesion} and shows a repeatability comparable to that of the semi-automatic whole-body approach of MTV_{total}. The Bland-Altman bias of $MTV_{subgroup}$ was -2.32 [95%CI: -5.81 – 1.17]. Supplemental Table 1 shows the association of RC with SUV_{max} RC decreasing with increasing minimum SUV_{max} of segmented lesions. This indicates that the repeatability is better when lesions with low SUV_{max} were discarded from the manually segmented subgroup of lesions.

Repeatability of semi-automatic segmentation of total tumor volume per patient

In total 1662 segmentations were performed for the *per patient* analysis, including segmentations for the 2 readers and 2 scans. The MTV_{total} for each reader for scan 1 and scan 2 is presented in **Table 1**. The RCs of the whole-body MTV_{total} and related metrics are shown separately for both readers in **Table 4**. The RC of MTV_{total} was 35.0% [95%CI:24.9 – 49.7%], the mean between the RCs for each reader (37% and 33%). Linear regression and Bland-Altman scatterplots for MTV_{total} and $meanSUV_{max}$ for scan 1 and scan 2 showed strong correlation ($P<0.001$, $R^2 = 0.99$) and no significant bias based on visual analysis (**Fig. 4**). The corresponding Bland-Altman bias of MTV_{total} was -6.70 [95%CI: -14.32 – 0.93]. RC of MTV_{total} and related metrics remained robust even when readers were hypothetically exchanged between scan timepoints with MTV_{total} 37.3% [95%CI:27.9 – 49.3%] (**Table 5**). A high correlation of MTV_{total} between scans for the same reader (ICC = 0.998; $p < 0.001$) and between readers for the same scan (ICC = 0.993; $p < 0.001$) was noted (**Fig. 5**). MTV_{total} shows moderate correlation with PSA values ($P<0.002$, $R^2=0.53$) (**Fig. 6**). Other metrics using the semi-automatic technique such as total $meanSUV_{max}$, total $meanSUV_{mean}$, and PSMA-

TL_{total} also showed improved repeatability as compared to individual lesion segmentation with RC ranging from 23.6-28.4%.

Discussion

PSMA PET is now widely used for monitoring of patients with prostate cancer (*5*,*6*,*17*,*18*). Especially for recurrent prostate cancer, PSMA PET has demonstrated high sensitivity and specificity for localizing prostate cancer cells in the body (*5*,*6*). Growing evidence suggests that PSMA PET is also a useful clinical tool in patients with more advanced prostate cancer (*19–21*).

Measures of total tumor volume and total uptake on PSMA PET have been described, but its use remains under debate in prostate cancer monitoring (*9*,*10*). Analogous to the tumor/node/metastasis (TNM) system, the molecular imaging TNM (miTNM) system has been proposed which scores extent of disease with regard to local tumor, regional lymph node metastases, bone metastases and other distant metastases. (*22*). Given the distinct biological aggressiveness and survival implications of various metastatic sites, the TNM-based system will likely remain an important prognostic tool in prostate cancer (*23*). However, progressive disease is not always accompanied by the occurrence of new metastases but also by enlargement of existing metastases, so the best assessment tools would therefore encompass both anatomic and total tumor volume, enabling consideration of both global disease status and aggressiveness of the involved sites. Studies have shown the prognostic value of PET volumetry and measures of total uptake. PSMA MTV_{total} of high volume disease is a statistically significant poor prognostic factor for overall survival and PSMA uptake of all metastases (SUV_{mean} per patient) improves prognostication of overall survival in patients treated with ^{177}Lu-lutetium-PSMA-617 therapy (*12*,*24–27*).

The recently proposed PSMA PET progression criteria recommend assuming progressive prostate cancer in the setting of 30% tumor volume increase (*8*). However, this threshold was chosen arbitrarily in the absence of volume-based PSMA repeatability data. Also, there are currently no

consensus recommendations for PSMA PET segmentation algorithms among the various approaches that have been proposed for quantifying the PSMA tumor volume (*9,10*). A necessary step towards use of PSMA PET for reliable monitoring of disease is development of reliable and efficient methods for measuring total disease burden and determination of their repeatability.

Our analysis of repeatability evaluated PET volumetric and uptake measures using three different approaches to segmentation: 1) manual segmentation of individual tumors, 2) manual selection of a subgroup of tumors per patient, and 3) semi-automatic segmentation of total tumor burden per patient. The repeatability of individual tumor volumes (MTV_{lesion}) was poor (RC 77%). An explanation may be that the reported wCV for SUV_{max} (12-14%, Pollard et al.) combined with a volumetric measurement where a small change in radius from the 50% SUV_{max} threshold results in a large change in volume, predictably results in large variability. Therefore, monitoring disease based on individual manually segmented tumors does not appear to be a reliable marker for treatment response. The repeatability for subgroup MTV_{mean} and total MTV_{mean} was RC 33% and 35%, respectively, which is similar to that reported in the literature for ^{18}F-FDG for other cancers (*28,29*). An MTV based on a larger sample of tumors or total tumor volume rather than individual tumors appears to be more reliable, likely because the noise sensitive SUV_{max}-based thresholds and resulting volume differences have both plus and minus biases across all lesions, resulting in a tendency to cancel out. Although robust, the method based on selection of a subgroup of tumors would be time-consuming in clinical practice and prone to bias in lesion selection. Due to the limited data available, no clear recommendation for a minimum number of lesions for the subgroup of lesions can be made; moreover, the repeatability of quantified volume is likely influenced by the characteristics of the chosen lesions (e.g. lesion size, tissue type, etc). MTV_{total} remains robust even when alternating readers between baseline and follow up scans, suggesting this method would

hold up in clinical practice where scans are not always read by the same person. Therefore the standardized semi-automatic segmentation method for MTV_{total} proposed by Seifert et al. which worked well in this study may be a solution (*9*). Future investigation should focus on the fully automatic analysis of PSMA PET scans in analogy to FDG PET approaches (*30*). MTV_{total} showed moderate correlation with PSA, suggesting that further assessment of this metric for use as a surrogate biomarker for disease status is warranted.

Besides volumetry, we evaluated SUV measures which showed repeatability similar to that reported by Pollard et al. We also evaluated PSMA-TL and PSMA-TLQ, metrics which integrate tumor volume and uptake analogous to total lesion glycolysis for ^{18}F-FDG. These metrics showed poor repeatability in individual lesions, but improved repeatability for the subgroup of tumors and total tumor burden, so warrant further investigation (*12*). Interestingly, PMA-TLQ had greater variability compared to PSMA-TL. This might be partly explained by the fact that the tumor volume is normalized with the relatively stable (i.e. high repeatability) SUV_{mean}. Thereby, changes in the tumor volume have a larger influence on the resulting composite metric.

The present study has some limitations. The patient number was relatively small, which might influence the translatability to a larger patient population. The results might not be directly translatable to other PSMA ligands, especially to those that are conjugates with non-gallium radioisotopes. The segmentation technique employed in this study may cause difficulties when single lesions are segmented separately in follow up scans or when confluent lesions occur (**Fig. 2**). However, manual user-dependent adjustments can eliminate those artifacts. Finally, the test-retest dataset was performed under carefully controlled conditions (e.g. assuring the same scanner for scan 1 and scan 2, minimizing variation in uptake time and dose) which does not reflect the potential variations encountered in the real-world clinic setting.

Conclusion

^{68}Ga-PSMA-HBED-CC PET-derived MTV_{total} with semi-automatic whole-body segmentation is highly repeatable and suitable for monitoring disease in advanced prostate cancer. Other methods evaluated in this study such as single lesion volumes and subgroup of lesions per patient are limited due to inferior repeatability (MTV_{lesion}) or labor intensiveness ($MTV_{subgroup}$). MTV_{total} therefore presents an efficient and robust means of monitoring disease longitudinally. A change in magnitude of MTV_{total} of greater than 35% can be viewed as real change in tumor status progression or response to therapy.

Disclosures

Janet H. Pollard has been an investigator for Progenics (Advanced Accelerator Applications) and Endocyte (Novartis) and has received compensation for work done for KEOSYS/Exini. No other potential conflict of interest relevant to this article was reported. Dr Hadaschik reports consulting or advisory role at ABX, Astellas Pharma; Bayer, Bristol-Myers Squibb, Janssen, Lightpoint Medical, Inc; Research funding from Astellas Pharma, Bristol-Myers Squibb, German Cancer Aid, German Research Foundation; Travel, accommodations, expenses from Astellas Pharma, AstraZeneca, Janssen. Wolfgang P. Fendler was a consultant for BTG, and he received fees from RadioMedix, Bayer, and Parexel outside of the submitted work.

Key Points

QUESTION: What is the estimated test-retest repeatability of whole-body total molecular tumor volume (MTV_{total}) for ^{68}Ga-PSMA-HBED-CC PET/CT in patients with metastatic prostate cancer?

PERTINENT FINDINGS: This study evaluated test-retest repeatability of semi-automatic segmentation of whole-body MTV_{total} showing coefficient of variation (wCV) of 12.7% and RC ±35%. Repeatability of manually segmented individual tumors (MTV_{lesion}) was poor, while repeatability of manually selected subgroup of tumors per patient ($MTV_{subgroup}$) was robust, but limited due to labor intensiveness.

IMPLICATIONS FOR PATIENT CARE: Understanding test-retest repeatability for metrics of metastatic disease burden is important for the development of ^{68}Ga PSMA HBED-CC PET/CT as a quantitative imaging biomarker. This study suggests that semi-automatically segmented whole-body MTV_{total} is an efficient and robust for monitoring disease status.

References

1. Siegel RL, Miller KD, Jemal A. Cancer statistics, 2020. *CA Cancer J Clin*. 2020;70:7-30.

2. Scher HI, Morris MJ, Stadler WM, et al. Trial design and objectives for castration-resistant prostate cancer: Updated recommendations from the prostate cancer clinical trials working group 3. *J Clin Oncol*. 2016;34:1402-1418.

3. Denmeade SR, Sokoll LJ, Dalrymple S, et al. Dissociation between androgen responsiveness for malignant growth vs. expression of prostate specific differentiation markers PSA, hK2, and PSMA in human prostate cancer models. *Prostate*. 2003;54:249-257.

4. Yuan TC, Veeramani S, Lin MF. Neuroendocrine-like prostate cancer cells: Neuroendocrine transdifferentiation of prostate adenocarcinoma cells. *Endocr Relat Cancer*. 2007;14:531-547.

5. Fendler WP, Calais J, Eiber M, et al. Assessment of 68Ga-PSMA-11 PET Accuracy in Localizing Recurrent Prostate Cancer: A Prospective Single-Arm Clinical Trial. *JAMA Oncol*. 2019;5:856-863.

6. Hofman MS, Lawrentschuk N, Francis RJ, et al. Prostate-specific membrane antigen PET-CT in patients with high-risk prostate cancer before curative-intent surgery or radiotherapy (proPSMA): a prospective, randomised, multicentre study. *Lancet*. 2020;395:1208-1216.

7. Fanti S, Goffin K, Hadaschik BA, et al. Consensus statements on PSMA PET/CT response assessment criteria in prostate cancer. *Eur J Nucl Med Mol Imaging*. 2020.

8. Fanti S, Hadaschik B, Herrmann K. Proposal for systemic-therapy response-assessment

criteria at the time of PSMA PET/CT imaging: The PSMA PET progression criteria. *J Nucl Med*. 2020;61:678-682.

9. Seifert R, Herrmann K, Kleesiek J, et al. Semi-automatically quantified tumor volume using Ga-68-PSMA-11-PET as biomarker for survival in patients with advanced prostate cancer. *J Nucl Med*. April 2020:10.2967/jnumed.120.242057.

10. Gafita A, Bieth M, Krönke M, et al. qPSMA: Semiautomatic Software for Whole-Body Tumor Burden Assessment in Prostate Cancer Using 68 Ga-PSMA11 PET/CT . *J Nucl Med*. 2019;60:1277-1283.

11. Grubmüller B, Senn D, Kramer G, et al. Response assessment using 68 Ga-PSMA ligand PET in patients undergoing 177 Lu-PSMA radioligand therapy for metastatic castration-resistant prostate cancer. *Eur J Nucl Med Mol Imaging*. 2019;46:1063-1072.

12. Seifert R, Kessel K, Schlack K, et al. PSMA PET total tumor volume predicts outcome of patients with advanced prostate cancer receiving [177Lu]Lu-PSMA-617 radioligand therapy in a bicentric analysis. *Eur J Nucl Med Mol Imaging*. 2020.

13. Pollard JH, Raman C, Zakharia Y, et al. Quantitative Test-Retest Measurement of 68Ga-PSMA-HBED-CC in Tumor and Normal Tissue. *J Nucl Med*. 2020;61:1145-1152.

14. Boellaard R, Delgado-Bolton R, Oyen WJG, et al. FDG PET/CT: EANM procedure guidelines for tumour imaging: version 2.0. *Eur J Nucl Med Mol Imaging*. 2015;42:328-354.

15. Bland JM, Altman DG. Statistical methods for assessing agreement between two methods of clinical measurement. *Lancet (London, England)*. 1986;1:307-10.

16. Obuchowski NA. Interpreting Change in Quantitative Imaging Biomarkers. *Acad Radiol*. 2018;25:372-379.

17. Rahbar K, Afshar-Oromieh A, Jadvar H, Ahmadzadehfar H. PSMA Theranostics: Current Status and Future Directions. *Mol Imaging*. 2018;17:1536012118776068.

18. Rahbar K, Weckesser M, Ahmadzadehfar H, Schafers M, Stegger L, Bogemann M. Advantage of (18)F-PSMA-1007 over (68)Ga-PSMA-11 PET imaging for differentiation of local recurrence vs. urinary tracer excretion. *Eur J Nucl Med Mol Imaging*. 2018;45:1076-1077.

19. Fendler WP, Weber M, Iravani A, et al. Prostate-Specific Membrane Antigen Ligand Positron Emission Tomography in Men with Nonmetastatic Castration-Resistant Prostate Cancer. *Clin Cancer Res*. 2019;25:7448-7454.

20. Farolfi A, Hirmas N, Gafita A, et al. PSMA-PET identifies PCWG3 target populations with superior accuracy and reproducibility when compared to conventional imaging: a multicenter retrospective study.; 2020.

21. Weber M, Kurek CE, Barbato F, et al. PSMA-ligand PET for early castration-resistant prostate cancer: a retrospective single-center study. *J Nucl Med*. 2020;57:jnumed.120.245456.

22. Eiber M, Herrmann K, Calais J, et al. Prostate cancer molecular imaging standardized evaluation (PROMISE): Proposed miTNM classification for the interpretation of PSMA-ligand PET/CT. *J Nucl Med*. 2018;59:469-478.

23. Halabi S, Kelly WK, Ma H, et al. Meta-analysis evaluating the impact of site of metastasis

on overall survival in men with castration-resistant prostate cancer. *J Clin Oncol*. 2016;34:1652-1659.

24. Kyriakopoulos CE, Chen Y-H, Carducci MA, et al. Chemohormonal Therapy in Metastatic Hormone-Sensitive Prostate Cancer: Long-Term Survival Analysis of the Randomized Phase III E3805 CHAARTED Trial. *J Clin Oncol*. 2018;36:1080-1087.

25. Chi KN, Agarwal N, Bjartell A, et al. Apalutamide for Metastatic, Castration-Sensitive Prostate Cancer. *N Engl J Med*. 2019;381:13-24.

26. Sweeney CJ, Chen Y-H, Carducci M, et al. Chemohormonal Therapy in Metastatic Hormone-Sensitive Prostate Cancer. *N Engl J Med*. 2015;373:737-746.

27. Seifert R, Seitzer K, Herrmann K, et al. Analysis of PSMA expression and outcome in patients with advanced Prostate Cancer receiving 177 Lu-PSMA-617 Radioligand Therapy. *Theranostics*. 2020;10:7812-7820.

28. Kramer GM, Frings V, Hoetjes N, et al. Repeatability of Quantitative Whole-Body 18F-FDG PET/CT Uptake Measures as Function of Uptake Interval and Lesion Selection in Non-Small Cell Lung Cancer Patients. *J Nucl Med*. 2016;57:1343-9.

29. Kruse V, Mees G, Maes A, et al. Reproducibility of FDG PET based metabolic tumor volume measurements and of their FDG distribution within. *Q J Nucl Med Mol Imaging*. 2015;59:462-8.

30. Sibille L, Seifert R, Avramovic N, et al. 18 F-FDG PET/CT Uptake Classification in Lymphoma and Lung Cancer by Using Deep Convolutional Neural Networks. *Radiology*. December 2019:191114.

Figures

Figure 1

Semi-automatic total tumor segmentations with red overlay designating sites of segmented lesions in scan 1 and scan 2 for two patients with disease limited to the prostate and left pelvic lymph nodes (A) and extensive skeletal metastases (B). The interval between the scans was 2 days for both patients.

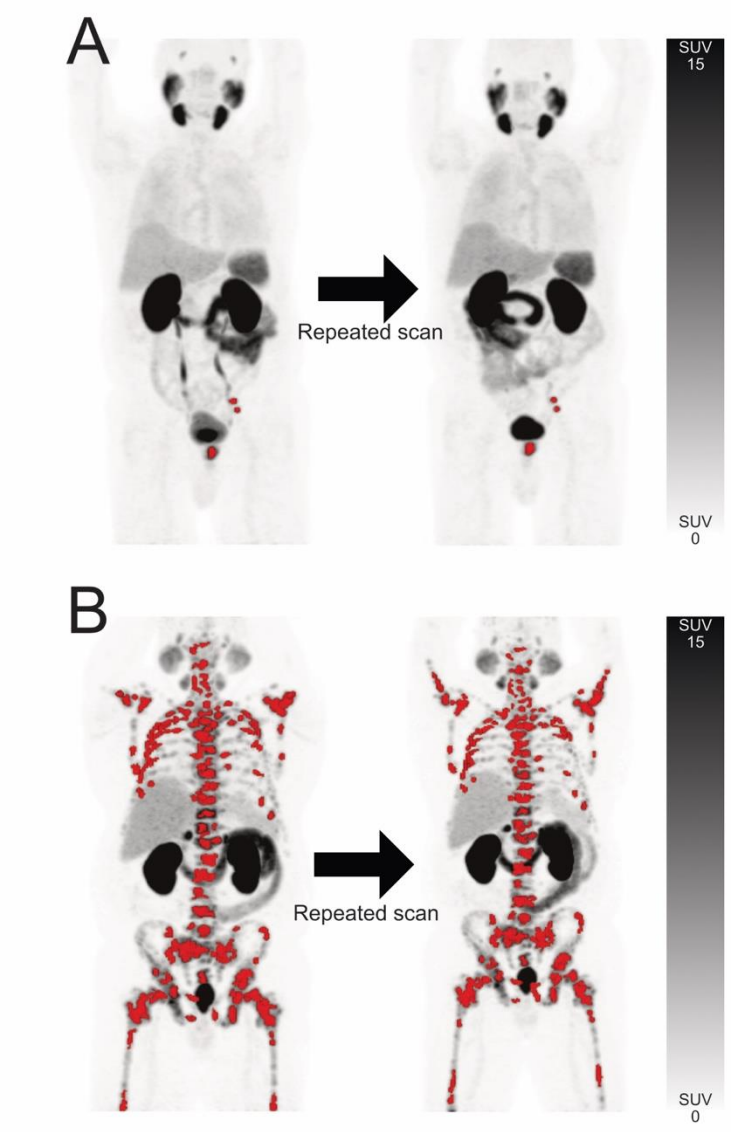

Figure 2

Example cases of segmentation challenges on ^{68}Ga-PSMA-HBED-CC PET/CT. Segmented tumor metastases are shown in red. (A) A metastasis in the os ilium was segmented as a single lesion on the first scan, but as three separate lesions in second scan (green circle). (B) A metastasis in the rib was segmented accurately on first scan, but inaccurately on the second scan with the isocontour including a portion of the lung (green circle). The error was resolved manually.

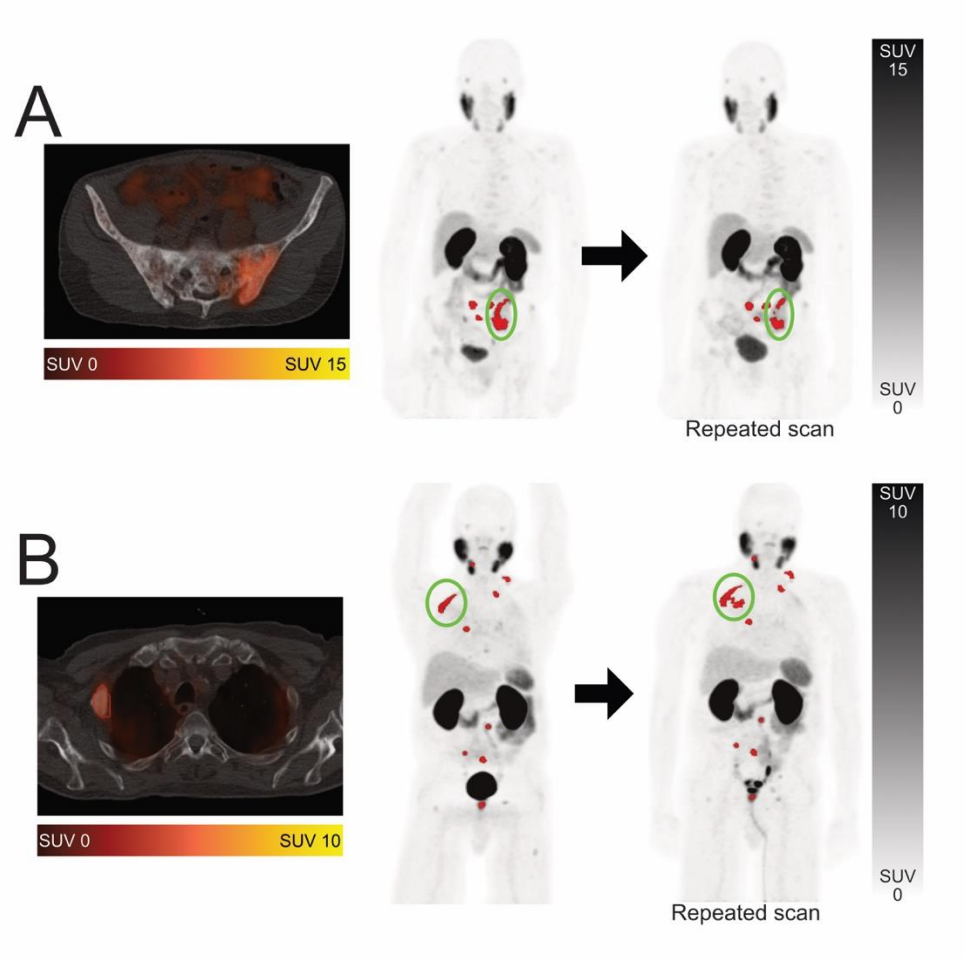

Figure 3

Analysis of individual manually segmented ^{68}Ga-PSMA-HBED-CC-avid lesions. Linear regression and Bland-Altman plots (A and B) of MTV_{lesion} show correlation between scans. (C) An association is noted between MTV_{lesion} and SUV_{max} changes between scan 1 and scan 2.

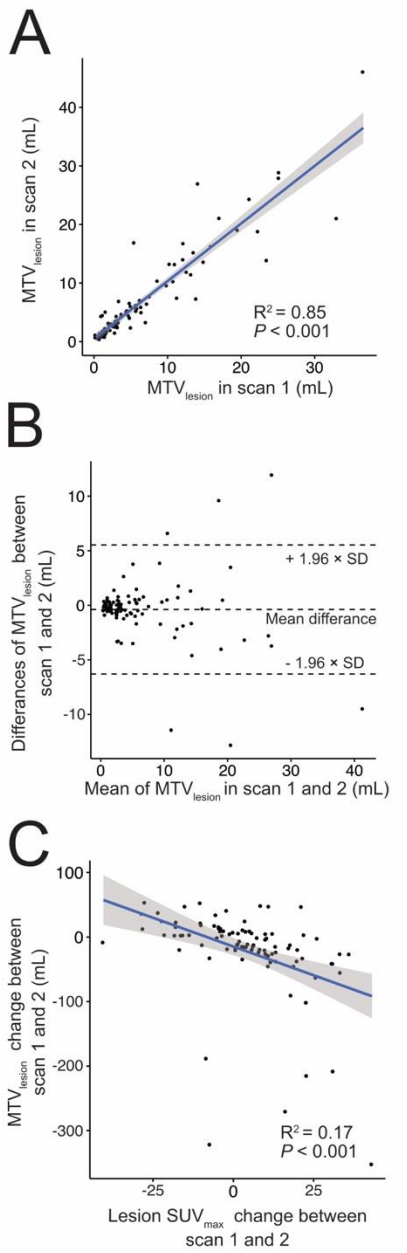

Figure 4

Analysis of semi-automatic whole-body segmentation of ^{68}Ga-PSMA-HBED-CC-avid lesions. Linear regression (A and C) and Bland-Altman plots (B and D) of MTV_{total} and $meanSUV_{max}$ show excellent correlation between scans and suggest no association between total tumor volume or lesion intensity and test-retest differences. Results for reader 1 and reader 2 were averaged for the purposes of these graphs. (A and C) MTV_{total} and $meanSUV_{max}$ for scan 1 are each plotted separately against the same metric for scan 2. (B and D) The mean of MTV_{total} or $meanSUV_{max}$ between scan 1 and scan 2 was plotted against the absolute difference in the metric between the two scans.

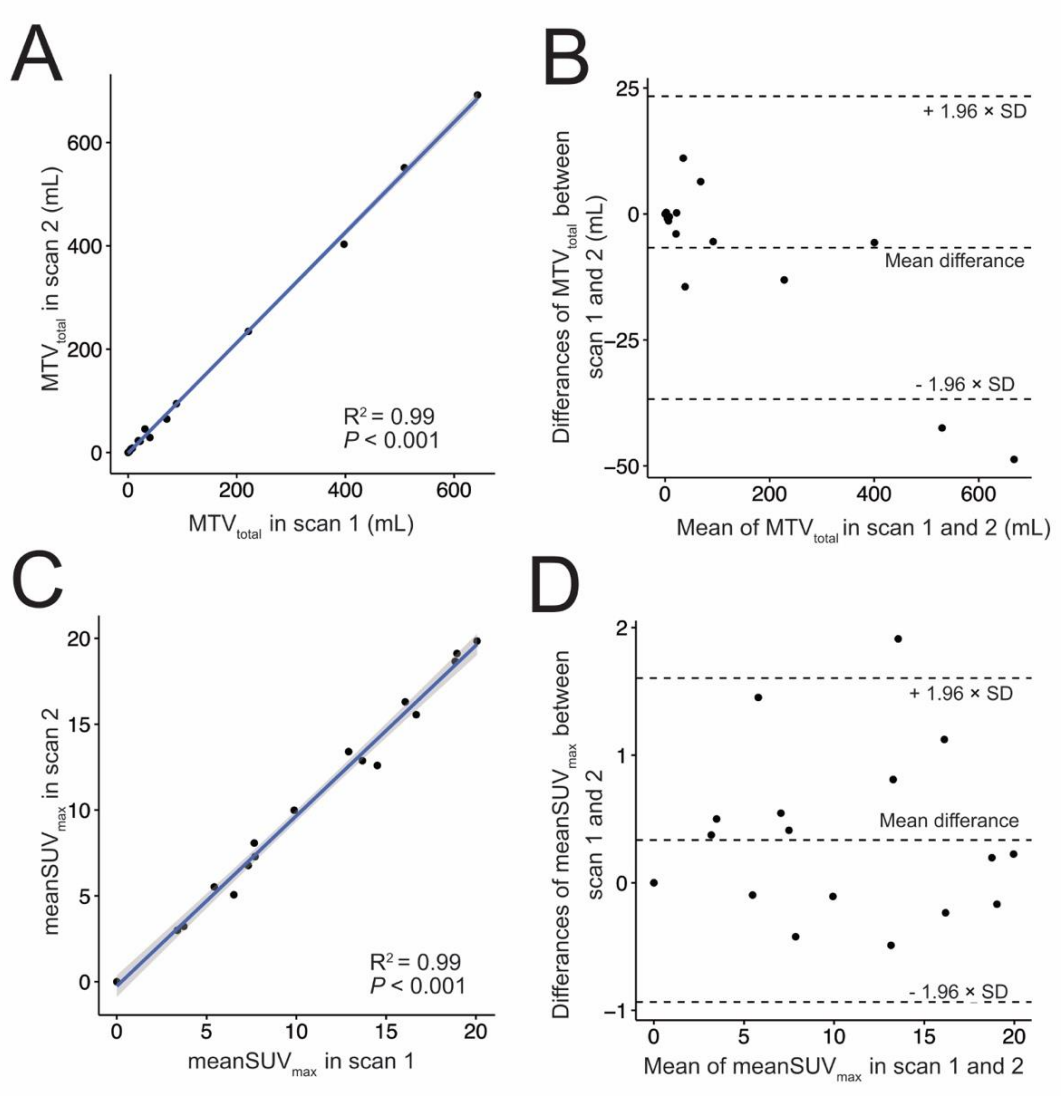

Figure 5

Graphical analysis of intra- and inter-reader agreement in reporting MTV_{total} with (A) showing high correlation in measures between scan 1 and scan 2 for the same reader (Reader 1), and (B) showing high correlation in measures between the two independent readers for the same scan (scan 1).

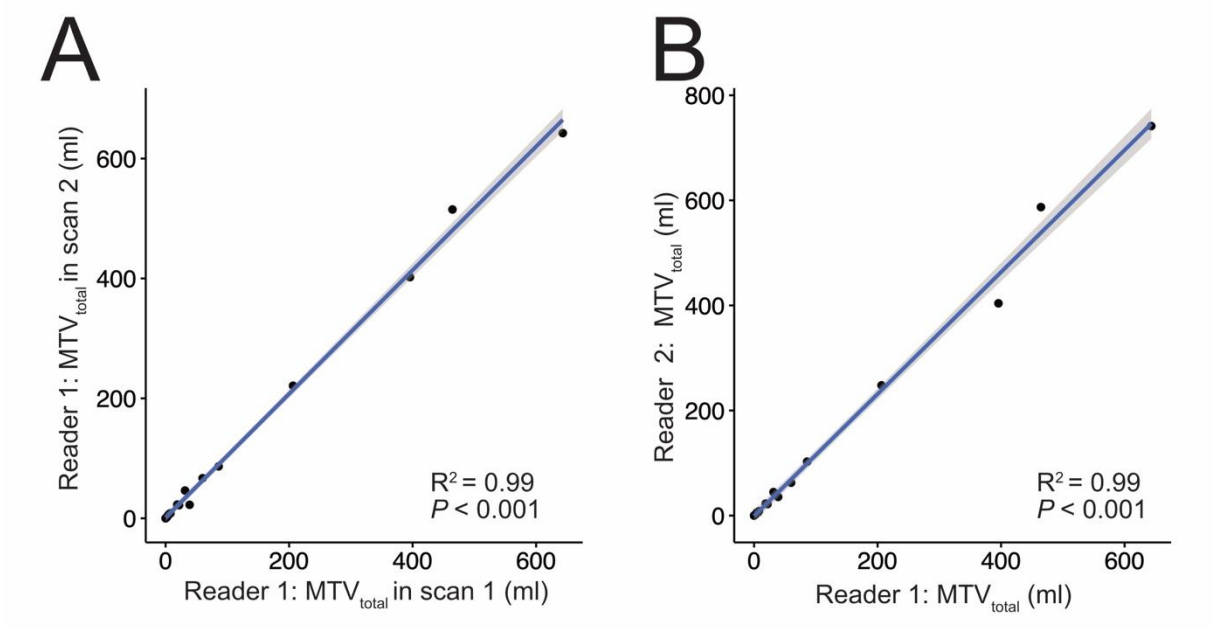

Figure 6

Graphical analysis of PSA versus MTV_{total} with log-log plot showing moderate correlation.

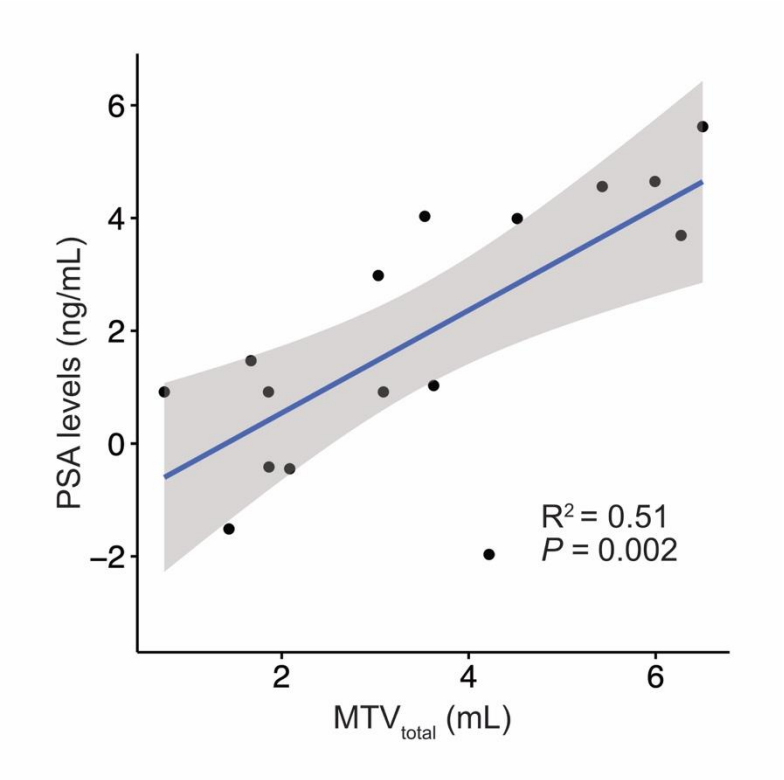

Tables

Table 1

Patient characteristics and MTV_{total} reported for each scan and reader

Patient	PSA within ≤90 d (ng/mL)	Gleason score at diagnosis	MTV_{total} (mL)			
			R1, Scan 1	R2, Scan 1	R1, Scan 2	R2, Scan 2
1	0.15	7(4 +5)	0	0	0	0
2	4.35	6(3+3)	4.81	5.88	4.81	5.88
3	104.5	9(4+5)	395.7	404.02	399.18	402.22
4	0.14	9(4+5)	59.91	62.59	82.42	66.9
5	0.66	9(5+4)	6.42	6.77	5.18	7.56
6	0.22	9(5+4)	3.78	4.67	3.78	4.67
7	56.3	Presumptive diagnosis	38.89	35.59	41.36	22.49
8	95.5	7(4+3)	206.38	247.85	236.35	221.08
9	276.3	9(4+5)	643.19	741.4	643.19	642.43
10	0.04	Presumptive diagnosis	0	0	0	0
11	0.64	9(4+5)	7.78	8.33	7.78	8.33
12	2.8	Lymph node biopsy	31.49	44.68	30.53	46.24
13	40.1	10(5+5)	464.53	587.13	552.7	515.05
14	19.7	7(3+4)	18.87	22.83	18.87	22.83
15	2.5	Bone biopsy	2.26	1.96	2.26	1.96
16	54.1	9(5+4)	85.89	102.6	92.3	86.56
17	2.5	9(5+4)	21.78	21.81	22.29	21.81
18	2.5	9(5+4)	6.52	6.31	5.53	7.34

R1 = reader 1, R2 = reader 2

Table 2
Repeatability of manually segmented individual lesions (MTV_{lesion})

Metric	wCV (%)	RC (%)	95% CI of RC (%)
MTV_{lesion}	27.7	76.9	62.9 – 95.9
PSMA-TL_{lesion}	23.3	64.7	53.4 – 80.67
PSMA-TLQ_{lesion}	34.5	95.7	81.5 – 114.5
Lesion SUV_{max}	12.4	34.4	29.6 – 41.2
Lesion SUV_{peak}	9.9	27.3	23.3 – 32.8
Lesion SUV_{mean}	11.8	32.7	27.5 – 40.2

wCV = coefficient of variation, RC = repeatability coefficient, CI = confidence interval.

Table 3

Repeatability of manually selected lesion subgroup per patient ($MTV_{subgroup}$)

Metric	wCV (%)	RC (%)	95% CI of RC
$MTV_{subgroup}$	12.0	33.1	24.2 – 46.2
Subroup MTV_{mean}	12.0	33.1	24.8 – 47.7
$PSMA\text{-}TL_{subgroup}$	7.4	20.6	16.0 – 26.9
$PSMA\text{-}TLQ_{subgroup}$	18.4	51.0	36.5 – 78.0
Subgroup $meanSUV_{max}$	12.3	34.0	20.0 – 59.4
Subgroup $meanSUV_{peak}$	6.6	18.3	13.3 – 24.5
Subgroup $meanSUV_{mean}$	9.1	25.2	17.5 – 35.7

wCV = coefficient of variation, RC = repeatability coefficient, CI = confidence interval.

Table 4
Repeatability of semi-automatic total tumor volume (MTV_{total}) per patient

Metric	R1 wCV (%)	R2 wCV (%)	Mean wCV (%)	R1 RC (%)	R2 RC (%)	Mean RC (%)	95% CI of mean RC
MTV_{total}	13.4	11.9	12.7	37.0	33.0	35.0	24.9 – 49.7
Total MTV_{mean}	13.4	11.9	12.7	37.1	33.0	35.0	25.0 – 48.8
$PSMA\text{-}TL_{total}$	8.4	12.1	10.3	23.3	33.5	28.4	20.7 – 41.9
$PSMA\text{-}TLQ_{total}$	19.4	17.3	18.4	53.9	48.0	50.9	32.7 – 84.7
Total $meanSUV_{max}$	8.4	8.6	8.5	23.3	23.9	23.6	17.0 – 32.4
Total $meanSUV_{mean}$	8.1	8.0	8.1	22.6	22.2	22.4	16.4 – 30.7

R1 = reader 1, R2 = reader 2, wCV = coefficient of variation, RC = repeatability coefficient, CI = confidence interval.

Table 5
Repeatability of MTV_{total} with different readers between scans

Metric	R1, R2 RC (%)	R2, R1 RC (%)	Mean RC (%)	95% CI of mean RC
MTV_{total}	29.9	44.7	37.3	27.9 – 49.3
Total MTV_{mean}	29.9	44.7	37.3	29.9 – 44.7
PSMA-TL_{total}	24.9	37.2	31.0	24.5 – 39.5
PSMA-TLQ_{total}	52.5	58.4	55.5	38.1 – 83.6
Total meanSUV_{max}	28.3	20.7	24.5	17.5 – 33.5
Total meanSUV_{mean}	27.4	18.7	23.1	17.2 – 31.1

R1, R2 = first scan read by reader 1, second scan read by reader 2; R2, R1 = first scan read by reader 2, second scan read by reader 1; wCV = coefficient of variation, RC = repeatability coefficient, CI = confidence interval.

Supplemental Table 1
Repetability of MTV_{lesion} with regard to SUV_{max}

Minimum SUV_{max} of the regarded lesions	RC%
1	76.9
6	62.8
11	57.0
16	44.5
21	49.3
26	53.1
31	10.7
36	12.2
41	12.2

Graphical Abstract